ZINC PECTINATE-*SESBANIA* GUM-MEDIATED INTERPENETRATING POLYMER NETWORK-BASED MICROBEADS AS A CANDIDATE FOR FLOATING DRUG DELIVERY OF ESOMEPRAZOLE

KIRTI RAJPUT,[*] SOPAN NANGARE,[**] SAGAR CHAUDHARI,[*] GANESH PATIL[*] and LAXMIKANT ZAWAR[*]

[*]*Department of Pharmaceutics, H. R. Patel Institute of Pharmaceutical Education and Research, Shirpur 425405, Maharashtra State, India*
[**]*Department of Pharmaceutical Chemistry, H. R. Patel Institute of Pharmaceutical Education and Research, Shirpur 425405, Maharashtra State, India*
✉ *Corresponding author: L. R. Zawar, shwet.zawar@gmail.com*

Received November 22, 2023

This study aimed to develop esomeprazole-loaded zinc-pectinate-*Sesbania* gum floating microbeads, optionally supplemented with calcium silicate, as a gastro-retentive drug delivery system. The microbeads were produced using the ionic gelation method, with zinc acetate as the crosslinking agent, and were characterized through *in vitro* studies. The findings revealed that all formulations exhibited high drug encapsulation efficiency and sustained drug release profiles. Polymer ratios, calcium silicate incorporation, and the choice of low-density oils significantly influenced drug encapsulation efficiency and release kinetics. Notably, the B:6 batch, formulated with *Sesbania* gum and low methoxy pectin, demonstrated outstanding performance, releasing 95.89 ± 1.66% of the drug within 7 h, with a floating lag time of 1.18 ± 0.07 min, indicating promising *in vitro* gastro-retention capabilities. Analysis of P-XRD, FT-IR, SEM, and DSC data highlighted changes in crystallinity, drug–excipient compatibility, surface morphology, and thermal behavior of esomeprazole and esomeprazole-loaded microbeads. In conclusion, these floating microbeads represent a potential gastro-retentive drug delivery system, offering enhanced buoyancy and prolonged drug release, with potential therapeutic advantages for peptic ulcer management.

Keywords: low methoxy pectin, *Sesbania* gum, calcium silicate, low-density oils, microbeads

INTRODUCTION

Natural polymers have been commonly employed in different pharmaceutical preparations, such as in matrix-controlled systems, mucoadhesive films, microparticles, coating agents, nanoparticles (NPs), high-viscosity formulations, such as eye drops, implantable devices, and suspensions.[1,2] Principally, due to their flexibility and efficacy, they have also been utilized as viscosity modifiers, stabilizing agents, suspending agents, solubilizers, emulsifying and gelling agents, bio-adhesives, disintegrants, as well as binding agents in various formulations.[3,4] It has been claimed that polymers, both synthetic and natural, have been intensively investigated and used in a variety of pharmacological applications.[5] Synthetic polymers have major drawbacks, such as high prices, toxic effects, contamination during the synthesis process, non-renewable sources, side effects, and poor patient acceptance.[6] As per the literature, natural polymers are appealing for pharmaceutical applications, because they are inexpensive, widely accessible, cost-effective, non-toxic, chemically modifiable, possibly biodegradable, with a few exceptions, and also demonstrate excellent biocompatibility.[7,8] Natural gums (plant-derived) are water-soluble and represent high-molecular-weight carbohydrate polymers composed of monosaccharides linked by glycosidic linkages. In most cases, natural gums show hydrophilic behavior and swelling when blended with cold water. Finally, they provide jelly or thick viscous solutions.[6] Based on this, the use of gums can be a great alternative for developing a novel carrier for drug delivery applications.

The oral drug delivery method has grown in popularity due to various attractive qualities, such as decreased therapy costs, ease of administration and greater patient compliance and acceptability.[9,10] It has been established that the medicine taken orally takes 1-2 h to go from the stomach to the intestine, and then it stays in the intestine for 14 to 24 h.[10,11] However, because of the short residence time in the stomach, drugs with an absorption window in the stomach suffer from considerable bioavailability problems and this can be overcome by preparing gastro-retentive drug delivery systems (GRDDSs).[12,13] According to previously published works, floating drug delivery systems are one of the available strategies that are recommended to be employed for extending the gastric retention time (GRT).[14,15] A gastro-retentive drug delivery system is excellent for medications having an absorption window in the stomach or upper gastrointestinal tract.

In recent investigations, sodium alginate, low methoxy (LM) pectin, tamarind gum, karaya gum, and other naturally occurring polymers have been used to create robust microbead systems as drug delivery vehicles.[16,17] Interestingly, pectin is a polymer found in plant cell walls,[18] with its backbone predominantly made up of linearly connected *α*-(1-4)-*D*-galacturonic acid residues that are interspersed with *α*-(1-2)-linked-L-rhamnopyranose residues. Partially methyl-esterified galacturonic acid residues are also present in pectin molecules. Pectin is frequently combined with other polymers to form bio-adhesive oral dosage forms. Low methoxy pectin, with a degree of esterification of <50%, may establish ionic cross-linkages with divalent metal cations (*e.g*., Zn^{+2}), forming compact pectin microbeads.[19,20] Although minimal drug trapping and early drug release were seen with pectin formulations because of their maximal solubility and swellability in the aqueous environment, this may be solved by combining two polymers.

Sesbania gum (SG) is a form of hydrocolloid that is often derived from the endosperm of *Sesbania grandiflora* (family *Leguminosae*) seeds, which contain a high amount of mucilage (33%). It is mainly composed of galactomannan, with fats and proteins in a small amount.[21] Galactomannans are widely distributed polysaccharides, with several properties, such as hydrophilicity, gelling, thickening, binding, emulsifying, suspending, and film-forming ability, which have attracted industrial and academic interest.[22] Galactomannans are non-ionic polysaccharides, soluble in water, and employed in the medicine and food industries.[22,23] It is mainly composed of chains that are *β*-(1-4)-D-mannopyranose (Man) units, with a side chain unit of *α*-(1-6)-*D*-galactopyranose (Gal), joined.[22,24] Also, it shows thermal and chemical stability. SG is readily soluble in water and has high viscosity. As a result, it finds use as an adhesive, thickening, and stabilizing agent in the pharmaceutical and food sectors.[25] Also, SG can be used as a floating agent in the pharmaceutical industry [SG-based SR drug delivery]. Hence due to their huge advantages, SG is used in combination with low methoxy pectin to form interpenetrating polymer network (IPN) microbeads.[26]

Peptic ulcers, gastroesophageal reflux disease, and other acid-related diseases and disorders are common in adult people and are associated with an increased risk of death.[27] A peptic ulcer is a type of lesion that affects the stomach, duodenum, or esophagus. Ulcers usually affect the whole gastrointestinal system, from the lining of the mouth to the rectal area.[28] Gastric acid and an enzyme (pepsin) are believed to be responsible for the pathogenesis of a peptic ulcer.[29] The mucous membrane is responsible for the protection of the stomach and other internal organs from acid and bacteria. Over-secretion of gastric acid damages the mucous membrane, allowing the bacteria *Helicobacter pylori* to enter the barrier, leading to internal infections like ulcers. As a result, in the instance of a peptic ulcer, both gastric acid and bacteria are responsible for the condition's onset.[29,30] In such cases, proton pump inhibitors (PPIs), including esomeprazole (ESO), omeprazole, lansoprazole *etc*., are effective medications and are a critical partner in antibiotic regimens. The PPIs lower intestinal acidity and boost the ability of antibiotics to kill *H. pylori*. The mechanism of action of PPIs in peptic ulcers is the reduction of acid secretion by suppressing the H^+/K^+-ATPase pump system in gastric parietal cells.[31,32]

A literature survey reported that the ESO is a proton pump inhibitor with a lot of promise for treating acid-related disorders. The IUPAC name of esomeprazole magnesium trihydrate is Bis-{5-methoxy-2-[(*S*)([4-methoxy-3,5-dimethyl-2-pyridinyl]-methyl)-sulfinyl]-1H-benzimidazol-1-yl} magnesium.[33] It is employed as a model medicine in this study, since it has a shorter half-life and also has greater absorption in the stomach (it only

absorbs in the proximal part of the small intestine). It has a plasma half-life ($t_{1/2}$) of 1-1.5 h, a plasma protein binding rate of 97%, and is significantly metabolized in the liver by the CYT enzyme system.[34]

According to prior research, due to pectin's high biodegradability, excellent biocompatibility, acceptable mechanical performance, and acid stability, pectinate-based floating microbeads have been produced as multiple-unit GRDDS.[35] Nevertheless, the pectin-based microbeads exhibited maximal solubility and swellability in an aqueous environment, resulting in poor trapping and early drug release.[19,36] Early literature has also shown that merging pectin with other polymers is a simple and efficient way to enhance the performance of pectin microbeads due to the formation of strong crosslinking between the polymers that helps to avoid problems of early drug release.[19,20,37] Several natural polymers have been mixed with low methoxy pectin to improve its performance in prolonged drug delivery. As a result of developing Zn^{+2}-pectinate-SG floating microbeads, it is feasible to achieve a longer stomach residence period with site-specific drug delivery.

In the present work, ESO-loaded Zn^{2+}-pectinate-SG-mediated floating microbeads were prepared for a GRDDS. In brief, microbeads were successfully synthesized utilizing the ionic gelation process, wherein zinc acetate acts as a crosslinking agent. Different spectroscopic characterizations were performed, including FTIR, PXRD, DSC, and SEM. In this study, polymer ratios, calcium silicate inclusion, and low-density oil showed a considerable effect on ESO encapsulation efficiency. Also, drug entrapment efficiency demonstrates the proportional relationship between polymers and calcium silicate concentration. Finally, the floating profile of the ESO-loaded Zn^{+2}-pectinate-SG-mediated floating microbeads was evaluated. In conclusion, a good floating profile and prolonged release of ESO were attained by ESO-loaded Zn^{+2}-pectinate-SG floating microbeads. Thus, these developed ESO-loaded Zn^{2+}-pectinate-SG floating microbeads can be recommended as a promising candidate for GRDDSs.

EXPERIMENTAL

Materials

Esomeprazole (Mylan Laboratories, India), low methoxy pectin (MW ~30,000–1,00,000 g/mol, degree of esterification: 63-66%, and degree of amidation: 20%, Loba Chemie Pvt. Ltd., India), *Sesbania* gum (Lucid Colloids Ltd.), calcium silicate (Loba Chemie Pvt. Ltd., India), olive oil (Loba Chemie Pvt. Ltd., India), sunflower oil (Laboratory Made), light liquid paraffin (Loba Chemie Pvt. Ltd., India), methanol (Loba Chemie Pvt. Ltd., India) and zinc acetate (ZA) (Loba Chemie Pvt. Ltd., India) were employed. Every ingredient was of analytical grade.

Formulation of ESO-loaded Zn^{+2}-pectinate-SG floating microbeads

The ionotropic emulsion gelation technique was used to create ESO-loaded Zn^{+2}-pectinate-SG floating microbeads augmented with and without calcium silicate. Simply, the appropriate amount of polymers was dissolved in 60 mL of deionized water, with constant agitation on a magnetic stirrer. ESO, low-density oils and calcium silicate were added according to the formulation table (Table 1). Then, the emulsion was homogenized at 5,000 rpm for 15 min at room temperature to ensure that the emulsion was stable. For all formulations, the drug-to-polymer ratio was maintained at 1:7 (Table 1). After that, a 5% zinc acetate solution was prepared and the emulsion was dropped into it using a 21-gauge size needle. Then, the prepared beads were introduced into the crosslinking solution for 25 min. Furthermore, they were filtered and rinsed three times with deionized water. The microbeads were dried overnight and preserved in suitable condition till required. The batches (B:1 to B:5) were all prepared in the same way, but with an absence of calcium silicate. Table 1 shows the compositions for the formulation of ESO-loaded Zn^{+2}-pectinate-SG floating microbeads.

Characterization of microbeads

Spectroscopic characterizations

Fourier transform infrared (FT-IR) spectra were measured using an FT-IR spectrometer at frequencies ranging from 400 to 4000 cm^{-1}. The sample was mixed with potassium bromide, at a 1:100 ratio. The IR spectral data of ESO, SG, pectin, calcium silicate and ESO-loaded microbeads were obtained.[17] Thermograms of the ESO, SG, pectin and ESO-loaded microbeads were obtained from a differential scanning calorimeter (DSC). DSC data were recorded throughout a wide range of temperature (50-300 °C), at a heating rate of 10 °C/min.[19] Despite this, PXRD was employed to investigate modifications in drug crystallinity of microbeads.

Table 1
Formulation table for ESO-containing Zn^{+2}-pectinate-SG floating microbeads

Ingredients	B:1	B:2	B:3	B:4	B:5	B:6	B:7	B:8
ESO (mg)	300	300	300	300	300	300	300	300
LM-pectin (mg)	1750	1575	1050	1575	1575	1575	1575	1575
SG (mg)	350	525	1050	525	525	525	525	525
Olive oil (mL)	2.50	2.50	2.50			2.50		
Sunflower oil (mL)				2.50			2.50	
Light liquid paraffin (mL)					2.50			2.50
Calcium silicate (mg)						300	300	300

An X-ray diffraction study was performed to study the crystallinity of ESO-loaded microbeads, SG, pectin, and ESO using an X-ray diffractometer. Polymers were scanned from a 5º to 80º diffraction angle (2θ).[16] Scanning electron microscopy with a 15 kV accelerating voltage was used to analyze the morphological characteristics of ESO-loaded microbeads. The study was carried out to observe the surface morphology of ESO-loaded microbeads, SG, pectin, and pure ESO.[19]

Microbead size and density measurement

The average size of 50 dried microbeads of all batches was measured using an optical microscopy method. In this method, the calibration of the eyepiece micrometer was done as per the standard procedure. Then, the dried microbeads were placed on a simple glass slide and observed under a microscope. The number of divisions of the micrometer occupied by each microbead was noted down, and the average particle size of the microbeads was calculated using Equation (1):

$$\text{Average particle size} = \sum nd/n \times \text{C.F.} \quad (1)$$

where 'n' is the number of microbeads, 'd' is the diameter of microbeads and C.F. is the calibration factor.

Density

Here, to determine the density of the microbeads, 1 g of microbeads were weighed accurately and transferred into a 10 mL measuring cylinder. The volume occupied by the microbeads was used to determine the density of the microbeads, as calculated by Equation (2):

$$\rho = M / V \quad (2)$$

where 'ρ' is the density of the microbeads (g/cm^3), 'M' is the mass/weight of microbeads (g), and 'V' is the volume occupied by the microbeads (mL or cm).

Drug entrapment efficiency

The drug entrapment efficiency (DEE) of the prepared floating microbeads was determined using the previously reported method.[20] At first, 0.1 g of dried ESO-loaded microbeads were crushed and dispersed in 100 mL of pH 1.2 hydrochloric acid buffer for 24 h at room temperature with constant agitation. The solution was then filtered, appropriate dilution was applied if necessary, and the filtrate was spectrophotometrically examined (Shimadzu/UV-1800, Japan) at 301 nm. Then, using Equation (3), the % DEE was computed:

$$DEE\ (\%) = Actual\ drug\ content\ /\ Theoretical\ drug\ content \times 100 \quad (3)$$

Drug content

In this study, 100 mg of dried microbeads were crushed and dissolved in 100 mL of pH 1.2 hydrochloric acid buffer. The volumetric flasks were left for 12 h to thoroughly mix on a shaker. The material was then passed through the filter paper, and the filtrate was spectrophotometrically (Shimadzu/UV-1800, Japan) evaluated for drug content at 301 nm.

In vitro *drug release study*

In this step, *in vitro* release of ESO was performed using a USP type II (paddle type) apparatus (Electrolab Dissolution Tester, EDT-08Lx). In brief, initially, ESO-loaded microbeads equivalent to 20 mg of the drug were taken and then subjected to simulated gastric fluid (pH 1.2 hydrochloric acid buffer). For the release study, 900 mL of pH 1.2 hydrochloric acid buffer was used, whereas the temperature of dissolution media was fixed at 37 ± 0.5 °C. The paddle rotation speed was programmed at 50 rpm. For drug release analysis, a 5 mL sample was collected from the dissolution vessel. Herein, sample collection was done at predefined time intervals, namely, 1, 2, 3, 4, 5, 6 up to 7 h; simultaneously, 5 mL fresh pH 1.2 hydrochloric acid buffer was added to maintain sink conditions. Finally, the collected samples were examined spectrophotometrically (Shimadzu/UV-1800, Japan) at 301 nm. The % drug release was calculated using the calibration curve of ESO in pH 1.2 hydrochloric acid buffer.

In vitro *buoyancy testing*

The *in vitro* floating studies followed a protocol that had been reported earlier, with some modifications.[38] For these tests, 50 mg of ESO-loaded microbeads were introduced in 900 mL of pH 1.2 hydrochloric acid buffer. The experiment was carried out using type II dissolution (paddle type) equipment, with the dissolution medium remaining at 37 ± 0.5 °C

and the paddle rotation speed regulated at 50 rpm. The time it took for the microbeads to rise to the surface of the buffer was recorded as floating lag time and the % of ESO-loaded microbeads that continued to float after 7 h was recorded as % buoyancy.

Swelling index

The swelling of the drug-loaded microbeads was examined in pH 1.2 hydrochloric acid buffer systems for 6 h. 50 mg of prepared ESO-loaded microbeads were submerged in 100 mL pH 1.2 hydrochloric acid buffer, and allowed to stand for a predefined time interval. The temperature of the simulated gastric fluid was maintained at 37 ± 0.5 °C. Then, the samples were taken off at pre-determined time intervals, such as 1, 2, 3, 4, 5, and 6 h, wiped with tissue paper to remove excess test fluid, and reweighed. The % swelling index was estimated using Equation (4):

$$\text{Swelling index } (\%t) = W_t - W_0/W_0 \times 100 \quad (4)$$

where W_0 and W_t are the weight of the microbeads at times '0' and '*t*'.

RESULTS AND DISCUSSION

The ionic gelation technique was employed in this work to create SG blended pectin-based microbeads, with and without calcium silicate. When polymers, ESO, and low-density oils were introduced into the cross-linking solution, the carboxyl group of pectin and the hydroxyl group of SG were immediately crosslinked with the cationic Zn^{+2} (zinc ion) moiety of zinc acetate to form a 3D network, which then led to the formation of gelled microspheres. Furthermore, zinc ions with a lower coordination number could create significant non-covalent interactions, such as hydrogen bonding and hydrophobic interactions between pectin molecules.[19,20] However, hydro-complexes of Zn^{+2} first originate at a greater pH, then are immediately crosslinked with the carboxyl (COO^-) group of pectin.[19]

Internal and external gelation techniques were used to prepare microbeads augmented with calcium silicate (B:6 to B:8) (Table 1). In internal gelation, the calcium ion of calcium silicate was slowly released and internally interacted with polymers, leading to the formation of intramolecular crosslinking between polymer chains. This whole process of internal crosslinking occurs before the hardening with zinc ions.[19,39] Furthermore, when calcium silicate was completely distributed in the polymer solution, it stabilized the W/O emulsion and viscosity synergism was observed. The creation of hydrogen bonds between the silanol moiety of calcium silicate and the carboxyl groups of the polymers might be responsible for viscosity synergism.[19,40]

FT-IR analysis

To study the drug-excipient interactions, the FT-IR spectra of pectin, SG, calcium silicate, ESO, and ESO-loaded microbeads (B:6) were observed (Fig. 1). A sharp stretch at 3400 cm^{-1} and 2937 cm^{-1} in pectin's FT-IR spectrum indicates the presence of N-H and C-H groups. Moreover, the low-intensity signals of esterified and non-esterified COOH groups were seen at 1745 cm^{-1} and 1647 cm^{-1}. SG exhibited a broad absorption band at 3608 cm^{-1}, which was due to the stretching mode of the O-H bond. The peaks around 1666 cm^{-1} could be due to the C=O stretching and carbonyl (C-O) stretching found at 1061 cm^{-1}, respectively. The IR spectra of calcium silicate showed stretching of Si-O-Si and O-H groups around 1068 cm^{-1} and 3500 cm^{-1}. The presence of ESO signals at 1197 cm^{-1}, 1367 cm^{-1}, and 3419 cm^{-1} was mainly due to the stretching of the C-O, S=O, and N-H groups. The spectrum of ESO-loaded microbeads revealed the elimination of the pectin peak at 1647 cm^{-1} and a significant reduction in the strength of the carboxy ion peak, which was displaced to a greater absorption peak at 1527 cm^{-1}. This indicates the development of Zn^{+2}-pectinate floating microbeads. The infrared spectra of the optimized formulation showed the characteristic peaks of the pure drug (ESO).

DSC analysis

The thermal behavior of ESO, SG, pectin, and ESO-loaded microbeads was examined by DSC (Fig. 2). The DSC was performed to find out the state and thermal degradation of the ESO-loaded microbeads. ESO, SG, and pectin have endothermic peaks at 166 °C, 65 °C, and 155 °C, respectively. The endothermic peak of ESO-loaded microbeads appeared on the DSC thermogram at 155 °C and 160 °C, with less sharpness and strength. The drug melting peak intensity decreased after loading into microbeads, indicating that the drug was entrapped in the polymer matrix. The drug's endothermic peak in floating microbeads also widened, as compared to the pure drug peak, which is likely related to an incomplete overlap with the endothermic peak associated with the polymer.[19]

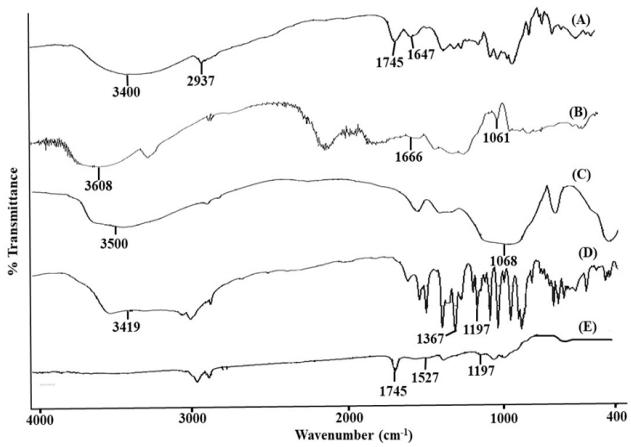

Figure 1: FT-IR spectra of pectin (A), SG (B), calcium silicate (C), ESO (D), and ESO-loaded microbeads (E) (B:6)

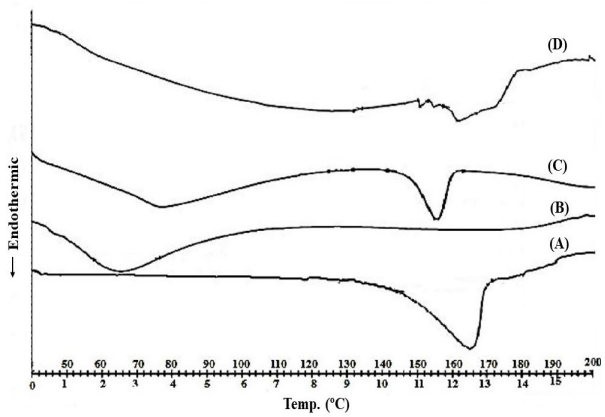

Figure 2: Thermograms of ESO (A), SG (B), pectin (C), ESO-loaded microbeads (D) (B:6)

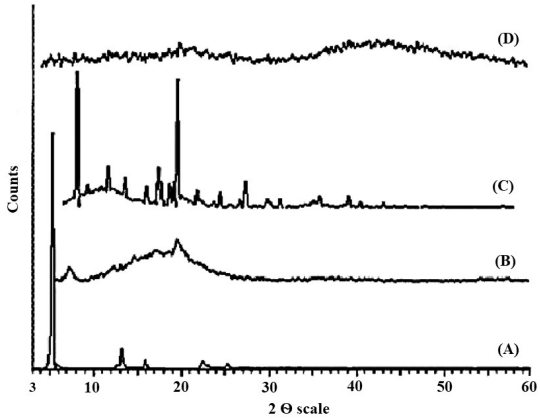

Figure 3: Diffractograms of ESO (A), SG (B), pectin (C), ESO-loaded microbeads (D) (B:6)

PXRD

Figure 3 presents the XRD spectra of ESO, SG, pectin, and ESO-loaded microbeads. The pure ESO peaks in Figure 3A were found to be at 5.20°, 13.10°, and 15.90° (2Θ), sharper and more intense, indicating the crystalline nature of the drug. In the case of SG (Fig. 3B), sharp peaks were found at 7.50° and 20.10° (2Θ). The XRD spectra of pectin (Fig. 3C) showed peaks at 8.10° and 20.70° (2Θ). The almost total elimination of characteristic peaks or a decrease in peak strength corresponding to the drug in the PXRD spectra of ESO-loaded microbeads (Fig. 3D) implies a conversion into an amorphous nature.

SEM

SEM images of ESO, pectin, SG, and ESO-loaded microbeads are shown in Figure 4. The ESO particles were found to be rough and irregular in shape (Fig. 4A). The shape of the pectin was found to be rough, and irregular with cracks (Fig. 4B). The SG particles had a strip, were smooth on the surface, and had an irregular particle size (Fig. 4C). The texture of ESO-loaded microbeads is somewhat spherical, with noticeable wrinkles and fissures (Fig. 4D). The microbeads also featured a hard skin, which might be attributed to the polymer-calcium silicate interfacial reactions.[41] The rough upper surface of the optimized microbeads had tiny holes or passages. These microscopic holes may have occurred as a result of escaping water at the time of dehydration and compression of the polymer networks.[19,20] The minor structural bending in microbeads could be caused by significant contraction of the polymer network due to the evaporation of entrapped water. A lack of ESO particles on the surface of such microbeads suggested that a drug had been properly distributed and incorporated into microbeads.[20] Some biopolymer material was also found on the surface of microbeads, which could have been generated as a result of the preparation technique. The number of oil compartments of varying sizes was visible on the surface, likely related to the

agglomeration of oily particles at the time of cross-linking activity.[16]

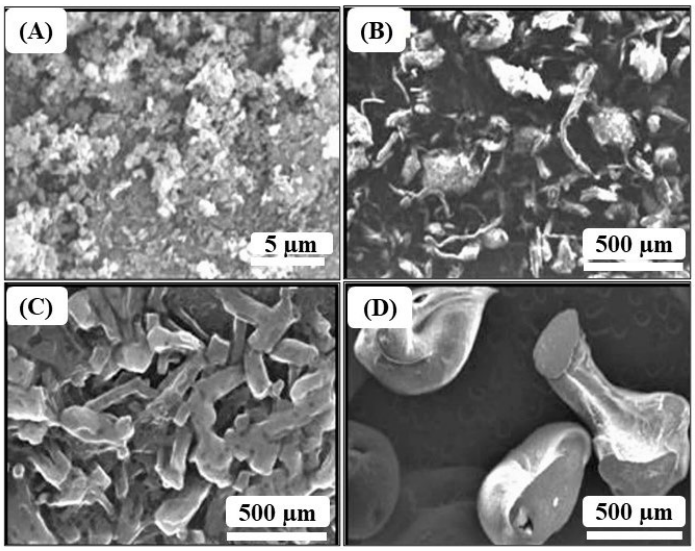

Figure 4: SEM images of ESO (A), pectin (B), SG (C), ESO-loaded microbeads (D) (B:6)

Table 2
Size, density, floating lag time, and % buoyancy of ESO-containing-Zn^{+2}-pectinate-SG microbeads

Formulation batches	Microbeads size (mm)	Microbeads density (g/cm^3)	Floating lag time (min)	% Buoyancy (7 h)
B:1	1.63 ± 0.14	0.783 ± 0.035	1.68 ± 0.16	21.09 ± 1.40
B:2	1.76 ± 0.08	0.761 ± 0.038	1.32 ± 0.15	31.89 ± 0.15
B:3	1.54 ± 0.05	0.660 ± 0.025	2.46 ± 0.08	70.03 ±1.33
B:4	1.80 ± 0.16	0.745 ± 0.040	2.28 ± 0.06	45.35 ± 1.45
B:5	1.71 ± 0.13	0.640 ± 0.043	3.08 ± 0.32	50.62 ±1.06
B:6	1.65 ± 0.06	0.807 ± 0.023	1.18 ± 0.07	57.00 ± 0.54
B:7	1.59 ± 0.05	0.880 ± 0.036	1.65 ± 0.36	34.35 ± 1.56
B:8	1.68 ± 0.14	0.914 ± 0.045	2.64 ± 0.15	40.80 ± 1.07

Mean ± S.D., n = 3

Size and density of microbeads

The desiccated Zn^{+2}-pectinate-SG microbeads had a particle size of 1.54 ± 0.05 mm to 1.80 ± 0.16 mm. Also, the density of the microbeads containing ESO was found to be between 0.647 ± 0.023 g/cm^3 to 0.914 ± 0.045 g/cm^3 (Table 2), which was less than the density of gastric acid. In this regard, the molecular structure of low methoxy pectin is mainly responsible for the greater size and lesser density of the produced microbeads.[19] A pectin molecule may form less tightly packed microbeads than sodium alginate particles. The rhamnose moiety of pectin often disrupts the cross-linking ability of the galacturonic acid moiety, making it lose, and the structural changes in the polymer may increase the entrapment of oil, which results in a decrease in microbead density.[19]

Also, the particle size of microbeads grows as the concentration of SG rises. Because the viscosity of the emulsion is directly related to SG concentration, the viscosity of the emulsion improves with a higher concentration of SG, resulting in larger particle size. Higher polymer concentration may lead to the development of thick dispersions, and the microbeads obtained from this dispersion are larger.[19] In short, the size of the microbeads increases with increasing biopolymer concentration. As compared to other formulation batches (B:2, B:5), the B:4 batch containing sunflower oil produced microbeads of larger diameter. The larger microbead size of B:4 may be due to delayed biopolymer dispersion penetration into the oil-water junction or an insufficient amount of dispersion to completely coat the oil-water junction formed during the gelation. Due to this, at the time of external gelation, the interfacial film between colliding particles gets disrupted and causes coalescence, which leads to a rise in microbead diameter.[19,39,42]

The addition of calcium silicate to the formulation greatly reduced the microbeads' size. This could be because calcium silicate has the potential to coagulate the suspended particles into firm microspheres by preventing membrane fouling and coalescence.[19,39,43] Furthermore, pectinate microbeads crosslinked with Ca^{+2} might inhibit its hydrophilic nature by stimulating intra-molecular hydrogen binding among amide groups, reducing microbead size.[19,44] The microbeads augmented with calcium silicate (B:6, B:7, and B:8) imparted increased density compared to the microbeads without calcium silicate (B:2, B:4, and B:5) because of their tight structure.[19]

Drug entrapment efficiency

The DEE of the microbeads containing ESO ranged from 65.15 ± 1.41% to 93.16 ± 0.86% (Table 3). It was most likely because of the quick development of the Zn^{+2}-crosslinked stiff polymeric network having compact surfaces that prevented drug loss from microbeads.[19,20,45] It was believed that the comparatively poor water solubility of ESO inhibited its outside migration from the microbeads. Furthermore, the addition of oils may produce an impermeable membrane, preventing drug molecules from eluting to the external media during formulation, resulting in increased DEE.[17,19] The formulation batch prepared by using sunflower oil (B:4) had a markedly higher DEE than the other formulations (B:2, B:4, and B:5). This could be related to the better dispersion of ESO particles in sunflower oil. Furthermore, as per the result, it was found that the formulation batch containing sunflower oil formed microbeads with a larger diameter and size, which could have more drug encapsulation possibilities. The larger size of microbeads (B:4) may further improve the drug's penetration path length, leading to little drug leakage from the microbeads.[19]

When the concentration of pectin in the biopolymer mixture was raised, drug entrapment inside microbeads was significantly increased. Because of its many anionic domains for ionotropic binding, it may compensate for the development of strong microbeads, resulting in reduced drug loss.[19,20,36] In this case, SG could operate as a viscosity-increasing mediator, extending the contact interval among interactive molecules, resulting in increased cross-linking sites and better pectin compaction. When correlated with other formulation batches (B:2, B:4, and B:5), the calcium silicate-containing formulations (B:6, B:7, and B:8) exhibited dramatically increased drug entrapment. This could be because the Ca^{+2} ions located on the surface of the pore-wall of calcium silicate could be electrostatically linked with ESO, which prevents the loss of the drug.[19] Furthermore, because of concomitant internal and external gel formation, the cross-linking strength in the calcium silicate-containing microbeads was increased and obstructing ESO diffusion at the time of formulation.[19,39] In comparison with the other batches, the B:6 batch exhibited high entrapment of 93.16%, while utilizing the same quantity of SG and pectin, which might be attributed to calcium silicate and oil type.

Table 3
DEE (%) and drug content (%) of ESO-containing-Zn^{+2}-pectinate-SG microbeads

Formulation batches	DEE (%)	Drug content (%)
B:1	80.56 ± 2.18	90.55 ± 0.005
B:2	75.16 ± 1.08	93.00 ± 0.008
B:3	90.5 ± 2.38	92.39 ±.019
B:4	91.3 ± 1.52	95.43 ± 0.004
B:5	78.9 ± 2.19	91.25 ± 0.014
B:6	93.16 ± 0.86	98.26 ± 0.003
B:7	84.13 ± 1.38	96.23 ±0.012
B:8	65.15 ± 1.41	94.12 ± 0.007

Mean ± S.D., n = 3

Drug content

The results of drug content are depicted in Table 3. The drug content of all formulations was in the range from 90.55 ± 0.005% to 98.26 ± 0.003%. The quick development of Zn^{+2}-biopolymer networks, with dense surfaces, limiting ESO loss from the microbeads, might improve DEE, resulting in the highest drug content.[19,20,45] The formulation batch prepared by using sunflower oil (B:4) had a markedly higher

drug content, as it had maximum entrapment efficiency, compared to the other formulations (B:2 and B:5). This might be related to the better dispersion of ESO particles in sunflower oil. However, as per the result, it was found that the formulation batch containing sunflower oil formed microbeads with a larger diameter and size, which could have more drug entrapment possibilities, and as the entrapment of the drug rises, the ESO content in the microbeads also increases.[19] When the concentration of pectin was increased, the drug content of microbeads was considerably improved by preventing drug leakage.

***In vitro* dissolution study**

Following 7 h, the % drug release of microbeads varied from 72.36 ± 1.12% to 95.89 ± 1.66% (Fig. 5). The most probable explanation for the prolonged drug release pattern could be that ESO particles (i) remained densely packed and scattered inside the emulsion particles, (ii) spread and encased inside the polymer chain system, resulting in the development of 3D microbeads. Drug transport from the microbeads to dissolving media was considered to occur in a two-step mechanism. The molecules first penetrate the polymer layer from the oil phase and then are conveyed outside the polymer layer into the dissolving media. This elongated the permeation route of ESO, resulting in prolonged drug release, without the first outburst issue.[17,19] Formulation batches with a higher polymer content may attach to water molecules more tightly, forming a sticky emulsion that might block all pore spaces of the microbeads, allowing for prolonged drug release.[20,36,37] Also, a greater level of polymer led to greater particle size microbeads, which resulted in a longer drug diffusional pathway. Furthermore, the zinc acetate-treated microbeads show smaller free volume and a higher degree of deformability, which could obstruct ESO inward mobility and slower drug dissolution and ultimately affect the drug release process.[20]

The release of drugs was drastically reduced when the concentration of pectin in the polymer composite was increased. In an acidic environment, the carboxy molecules of pectin could be protonated to generate water-insoluble pectinic acid. This might induce the shrinkage of floating microbeads, because of the breaking of electrostatic interactions and may show an ionic attraction and decreased ionic repulsion. At an acidic pH, hydrophobic linkages and hydrogen bonding were formed among pectin and SG. This could gradually block the openings on the microbead surface, allowing the drug release to be sustained.[19]

As compared to other low-density oils, olive oil-containing microbeads show slower drug release than others. In olive oil-containing microbeads (B:1), the polymers form a physically strong and thicker coating that might serve as a more capable protective layer to inhibit ESO penetration from the oil phase. The poor mechanical barriers created by sunflower oil in sunflower oil-entrapped microbeads (B:4) might be unable to impede ESO permeation, resulting in much faster drug liberation at 7 h.[19,42] However, the addition of calcium silicate considerably improved the release of the drug. The drug release might improve because an ion-exchange procedure can quickly remove the calcium ion attached to the surface of calcium silicate by one Si-OH molecule in the dissolving fluid that could disintegrate suddenly and break the silanol bonds.[19] Ultimately, the calcium silicate was dissolved, and the formation of pore spaces on microbeads with a higher drug release rate was observed.[19]

Among all formulation batches, the B:6 batch had the best drug solubility and dissolution pattern, with a drug release of 95.89 ± 1.66% over 7 h. To accomplish greater *in vivo* permeation and increased pharmacological effects of ESO, maximum drug absorption (~96%) of B:6 might be beneficial. The data indicates that the drug release from B6 was higher compared to the other batches. Consequently, B6 was selected as the optimized batch. The drug release data were fitted to various kinetic models, such as zero order, first order, Higuchi, Korsmeyer Peppas, and Hixson-Crowell models, to estimate the drug release mechanism followed by the formulations. From the results, it was found that most of the formulation batches followed the Higuchi release model as regression coefficient (R^2) was very close to 1 (Table 4). Here, the optimized batch B6 exhibited an R^2 value of 0.9911 for the Higuchi release model, surpassing other release kinetic models. In this context, drug release occurs as the polymer layer gradually disintegrates, allowing the drug to diffuse out from the microbeads. The release exponent (n) value for B:6 was determined to be 0.24, confirming that the designed formulation demonstrates a release exponent (n) of less than 0.45. This finding confirms that the drug diffusion mechanism from the designed

dosage form follows the Fickian diffusion-controlled release.

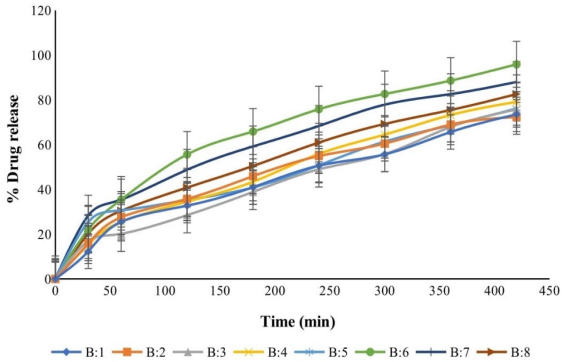

Figure 5: *In vitro* comparative drug release profiles of formulation batches B:1-B:8

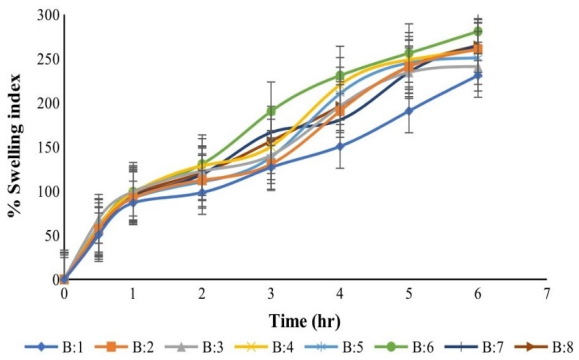

Figure 6: *In vitro* swelling study of formulation batches B:1-B:8

Table 4
Results of *in vitro* drug release data fitted to various release kinetic models (R^2)

Batches	Zero-order (R^2)	First-order (R^2)	Higuchi (R^2)	Korsmeyer-Peppas (R^2)	Hixson-Crowell (R^2)	Initial release rate (R_0)	Release exponent (n)
B:1	0.9818	0.891	0.9866	0.9795	0.9144	12.3	0.37
B:2	0.9717	0.8659	0.9955	0.9915	0.9112	15.86	0.36
B:3	0.9977	0.9665	0.9663	0.9666	0.9852	16.97	0.52
B:4	0.9898	0.9054	0.99	0.994	0.9453	15.32	0.38
B:5	0.9907	0.9869	0.9464	0.9283	0.9925	25.42	0.24
B:6	0.9387	0.821	0.9911	0.9888	0.8665	22.13	0.24
B:7	0.9746	0.9133	0.9975	0.9953	0.938	28.32	0.28
B:8	0.9832	0.9015	0.9972	0.9975	0.9369	20.16	0.31

Floating lag time (FLT) and % buoyancy

The buoyancy characteristic of ESO-loaded microbeads is shown in Table 2. The mean density of several microbeads was shown to be highly associated with buoyancy. All the preparations had a density that was less than that of the stomach content (1.004 g/cm^3), resulting in reduced FLT (less than 3.5 min). When low-density oils were added to the preparations, many tiny pouches formed on the inside of the microbeads, which was necessary for floating.[17,19] As time passed, water molecules began to penetrate into the microbeads over time, eventually taking the place of air, the density of the microbeads exceeded that of the gastric contents, and the microbeads slowly started to sink.[19] After 7 h, the microbeads had a % buoyancy from 21.09 ± 1.40% to 70.03 ± 1.33%.

As the concentration of pectin increased in the polymeric mixture, the buoyancy dropped drastically. That might be due to the structurally robust and dense construction of the Zn^{+2}-pectinate microbeads, which might shrink in acidic environments, leading to the microbead's density dropping much more. Low-density oils have no or little effect on the total buoyancy of microbeads. The porous structure of calcium silicate and their addition to the microbeads resulted in a significant rise in % buoyancy. The polymers formed liquid bridges over the calcium silicate surface to cover the pores, capturing air inside the pores and permitting the microbeads to bounce.[19,46] As a result, calcium silicate-loaded microbeads (B:6 to B:8) have a low density, which reduces floating lag time and boosts % buoyancy, increasing the swelling index.

Swelling index (SI)

The swelling characteristics of any polymer network are influenced by the characteristics of the polymeric material, the degree of cross-linking, and the suitability of the polymer for its solvent. The % swelling data (at 6 h) was found within the range of 230.96 ± 0.46% to 280.90 ± 0.15% (Fig. 6). The penetration of water into the polymeric microbeads induced by osmotic pressure increased swelling behavior during the early stages. This occurred due to massive

segmental mobility, which leads to increased length among polymer chains. The gradual degradation of the microbeads was responsible for the reduction in swelling after a certain period.[19]

As the concentration of pectin increases in a microbead formulation, the % swelling is reduced dramatically. This might be due to the Cl^- ion of acidic media, causing the de-crosslinking of the COOH group of pectin by the removal of zinc ions. As a result, the carboxyl group remained unionized. This reduced pore formation and microbead swelling, and in this way, the % swelling decreases as the polymer concentration increases.[19,20,47] The sunflower oil-containing microbeads (B:4) swelled more than the microbeads containing other oils (B:2 and B:5). Because the formulations containing sunflower oil (B:4) were less densely packed, allowing water to penetrate the polymer network more easily, causing them to swell more.[19] The addition of calcium silicate into the polymer blend could increase the swelling properties. The calcium silicate has a water-loving property that promotes the uptake of water and ultimately improves the swelling ability of polymers.[19,48]

CONCLUSION

This work explored the development of novel Zn^{+2}-pectinate-SG microbeads for intragastric ESO administration utilizing the floating approach. Herein, ESO-loaded microbeads were successfully prepared using the ionotropic gelation technique. The study found that the polymer composition, oil type (low-density), and calcium silicate addition significantly influenced drug encapsulation and the drug release profile. Batch B:6 had the maximum drug entrapment efficiency (DEE, 93.16 ± 0.86%) and maximum drug release at 7 h (Q7 h, 95.89%), as well as remarkable floating. The floating microbeads, which can be created quickly and easily, without the need for sophisticated processes or technical skills, offer significant potential for targeted hydrophobic drug delivery. The innovative floating microbeads would be packed in capsules to improve patient convenience. Furthermore, the aforementioned techniques have a high potential for industrial use.

ACKNOWLEDGMENTS: The authors address sincere thanks to the principal and management of H. R. Patel Institute of Pharmaceutical Education and Research, Shirpur, for providing all the required facilities for the completion of the research work.

REFERENCES

[1] N. Avramović, B. Mandić, A. Savić-Radojević and T. Simić, *Pharmaceutics*, **12**, 298 (2020), https://doi.org/10.3390/pharmaceutics12040298
[2] V. D. Prajapati, G. K. Jani, N. G. Moradiya and N. P. Randeria, *Carbohyd. Polym.*, **92**, 1685 (2013), https://doi.org/10.1016/j.carbpol.2012.11.021
[3] H. Lieberman, M. Rieger and G. S. Banker, "Pharmaceutical Dosage Forms: Disperse Systems", CRC Press, Boca Raton, 2nd ed., 2020, p. 555, https://doi.org/10.1201/9781003067368
[4] L. Gautam, A. Jain, P. Shrivastava, S. Vyas and S. P. Vyas, in "Polymeric and Natural Composites. Advances in Material Research and Technology", edited by M. S. Hasnain, A. K. Nayak and S. Alkahtani, Springer, Cham, 2022, pp. 1-24, https://doi.org/10.1007/978-3-030-70266-3_1
[5] X. Tong, W. Pan, T. Su, M. Zhang, W. Dong *et al.*, *React. Funct. Polym.*, **148**, 104501 (2020), https://doi.org/10.1016/j.reactfunctpolym.2020.104501
[6] L. N. V. Krishna, P. Kulkarni, M. Dixit, D. Lavanya and P. K. Raavi, *Int. J. Drug Formul. Res.*, **2**, 54 (2011)
[7] J. F. Resende, I. M. R. Paulino, R. Bergamasco, M. F. Vieira and A. M. S. Vieira, *Braz. J. Chem. Eng.*, **40**, 23 (2023), https://doi.org/10.1007/s43153-022-00224-8
[8] J. Liao and H. Huang, *Biomacromolecules*, **21**, 2574 (2020), https://doi.org/10.1021/acs.biomac.0c00566
[9] A. Choudhury, L. Renthlei, M. Dewan, R. Ahmed, H. Barakoti *et al.*, *J. Appl. Pharm. Res.*, **7**, 01 (2019), https://doi.org/10.18231/j.joapr.2019.003
[10] S. Thakur, K. Ramya, D. K. Shah and K. Raj, *J. Drug Deliv. Ther.*, **11**, 125 (2021)
[11] N. Pandey, N. Sah and K. Mahara, *Int. J. Pharm. Sci. Res.*, **7**, 453 (2016)
[12] V. D. Gaikwad, V. D. Yadav and P. D. Jadhav, *Asian J. Pharm.*, **6**, 245 (2014), https://doi.org/10.22377/ajp.v6i4.41
[13] S. S. Bisht, H. Chaurasia, S. Varshney and D. Kotiyal, *Int. J. Pharm. Sci. Res.*, **4**, 1912 (2013), http://dx.doi.org/10.13040/IJPSR.0975-8232.4(5).1912-17
[14] M. Calderón-Santoyo, M. Iñiguez-Moreno, J. C. Barros-Castillo, D. M. Miss-Zacarías, J. A. Díaz *et al.*, *Iran. Polym. J.*, **31**, 665 (2022), https://doi.org/10.1007/s13726-022-01033-z
[15] S. N. S. Anis, I. I. Muhamad, S. Selvakumaran, A. M. Marsin, W. C. Liew *et al.*, in "Ionically Gelled Biopolysaccharide Based Systems in Drug Delivery. Gels Horizons: From Science to Smart Materials", edited by A. K. Nayak, M. S. Hasnain and D. Pal, Springer, Singapore, 2021, pp. 161-185, https://doi.org/10.1007/978-981-16-2271-7_9

[16] H. Bera, S. G. Kandukuri, A. K. Nayak and S. Boddupalli, *Carbohyd. Polym.*, **120**, 74 (2015), https://doi.org/10.1016/j.carbpol.2014.12.009
[17] H. Bera, S. Boddupalli, S. Nandikonda, S. Kumar and A. K. Nayak, *Int. J. Biol. Macromol.*, **78**, 102 (2015), https://doi.org/10.1016/j.ijbiomac.2015.04.001
[18] J. Suksaeree, P. Maneewattanapinyo, K. Panrat, W. Pichayakorn and C. Monton, *J. Polym. Environ.*, **29**, 3174 (2021), https://doi.org/10.1007/s10924-021-02108-3
[19] H. Bera, J. Nadimpalli, S. Kumar and P. Vengala, *Int. J. Biol. Macromol.*, **104**, 1229 (2017), https://doi.org/10.1016/j.ijbiomac.2017.07.027
[20] H. Bera, S. Boddupalli and A. K. Nayak, *Carbohyd. Polym.*, **131**, 108 (2015), https://doi.org/10.1016/j.carbpol.2015.05.042
[21] S. Bunma and H. Balslev, *The Botanical Review*, **85**, 185 (2019), https://link.gale.com/apps/doc/A600446965/AONE?
[22] R. Li, X. Jia, Y. Wang, Y. Li and Y. Cheng, *Food Hydrocoll.*, **90**, 35 (2019), https://doi.org/10.1016/j.foodhyd.2018.11.048
[23] P. Vilaró, Z. Bennadji, E. Budelli, G. Moyna, L. Panizzolo *et al.*, *Food Hydrocoll.*, **77**, 711 (2018), https://doi.org/10.1016/j.foodhyd.2017.10.038
[24] Y. López-Franco, C. Cervantes-Montaño, K. Martínez-Robinson, J. Lizardi-Mendoza and L. Robles-Ozuna, *Food Hydrocoll.*, **30**, 656 (2018), https://doi.org/10.1016/j.foodhyd.2012.08.012
[25] K. A. Kumar, R. K. Ramakrishnan, M. Černík and V. V. Padil, "Micro-and Nanoengineered Gum-Based Biomaterials for Drug Delivery and Biomedical Applications", Elsevier, 2022, pp. 383-407, https://doi.org/10.1016/B978-0-323-90986-0.00008-X
[26] M. K. Yazdi, M. R. Ganjali, M. Rezapour, P. Zarrintaj, S. Habibzadeh *et al.*, in "Ionically Gelled Biopolysaccharide Based Systems in Drug Delivery. Gels Horizons: From Science to Smart Materials", edited by A. K. Nayak, M. S. Hasnain and D. Pal, Springer, Singapore, 2021, pp. 121-133, https://doi.org/10.1007/978-981-16-2271-7_7
[27] M. Alai and W. J. Lin, *Int. J. Nanomed.*, **10**, 4029 (2015), https://doi.org/10.2147/IJN.S82366
[28] H. Ardalani, A. Hadipanah and A. Sahebkar, *Mini-Rev. Med. Chem.*, **20**, 662 (2020), http://dx.doi.org/10.2174/1389557520666191227151939
[29] L. S. Goodman, "The Pharmacological Basis of Therapeutics", McGraw-Hill, New York, 1996, https://accessmedicine.mhmedical.com/book.aspx?bookID=3191
[30] E. Sverdén, L. Agréus, J. M. Dunn and J. Lagergren, *BMJ*, **367**, l5495 (2019), http://dx.doi.org/10.1136/bmj.l5495
[31] K. Tripathi, "Essentials of Medical Pharmacology", JP Medical Ltd., 2013
[32] V. Dipasquale, G. Cicala, E. Spina and C. Romano, *Front. Pharmacol.*, **13**, 839972 (2022), https://doi.org/10.3389/fphar.2022.839972
[33] M. Sanad, H. Eyssa, N. Gomaa, F. Marzook and S. Bassem, *Radiochim. Acta*, **109**, 711 (2021), https://doi.org/10.1515/ract-2021-1056
[34] S. Goel, V. Agarwal and M. Sachdeva, *Nanosci. Nanotechnol. - Asia*, **10**, 909 (2020), http://dx.doi.org/10.2174/2210681209666191111113850
[35] A. K. Nayak and D. Pal, *Int. J. Biol. Macromol.*, **62**, 137 (2020), https://doi.org/10.1016/j.ijbiomac.2013.08.020
[36] A. K. Nayak, D. Pal and K. Santra, *Carbohyd. Polym.*, **101**, 220 (2014), https://doi.org/10.1016/j.carbpol.2013.09.024
[37] A. K. Nayak, D. Pal and K. Santra, *Int. J. Biol. Macromol.*, **66**, 203 (2014), https://doi.org/10.1016/j.ijbiomac.2014.02.023
[38] I. U. Khan, M. Shoukat, M. Asif, S. H. Khalid, S. Asghar *et al.*, *Microorganisms*, **10**, 1171 (2022), https://doi.org/10.3390/microorganisms10061171
[39] H. Song, W. Yu, M. Gao, X. Liu and X. Ma, *Carbohyd. Polym.*, **96**, 181 (2013), https://doi.org/10.1016/j.carbpol.2013.03.068
[40] S. Puttipipatkhachorn, T. Pongjanyakul and A. Priprem, *Int. J. Pharm.*, **293**, 51 (2005), https://doi.org/10.1016/j.ijpharm.2004.12.006
[41] Y. Kawano, S. Chen and T. Hanawa, *Pharmaceutics*, **13**, 767 (2021), https://doi.org/10.3390/pharmaceutics13060767
[42] V. Castel, A. C. Rubiolo and C. R. Carrara, *Food Hydrocoll.*, **63**, 170 (2017), https://doi.org/10.1016/j.foodhyd.2016.08.039
[43] V. Zanatta, K. Rezzadori, F. M. Penha, G. Zin, E. Lemos-Senna *et al.*, *J. Food Eng.*, **195**, 73 (2017), https://doi.org/10.1016/j.jfoodeng.2016.09.025
[44] C. Dhalleine, A. Assifaoui, B. Moulari, Y. Pellequer, P. Cayot *et al.*, *Int. J. Pharm.*, **414**, 28 (2011), https://doi.org/10.1016/j.ijpharm.2011.04.059
[45] R. V. Kulkarni, S. Mutalik, B. S. Mangond and U. Y. Nayak, *J. Pharm. Pharmacol.*, **64**, 530 (2012), https://doi.org/10.1111/j.2042-7158.2011.01433.x
[46] R. H. Fahmy, *AAPS PharmSciTech*, **13**, 990 (2012), https://doi.org/10.1208/s12249-012-9823-2
[47] R. Singh, S. Maity and B. Sa, *Carbohyd. Polym.*, **106**, 414 (2014), https://doi.org/10.1016/j.carbpol.2014.01.033
[48] S.-M. Li, N. Jia, J.-F. Zhu, M.-G. Ma and R.-C. Sun, *Carbohyd. Polym.*, **80**, 270 (2010), https://doi.org/10.1016/j.carbpol.2009.11.024